



The application of artificial neural networks in the prediction of microemulsion phase boundaries in PEG-8 caprylic/capric glycerides based systems

Ljiljana Djekic*, Svetlana Ibric, Marija Primorac

Department of Pharmaceutical Technology and Cosmetology, Faculty of Pharmacy, Vojvode Stepe 450, P.O. Box 146, 11221 Belgrade, Serbia

ARTICLE INFO

Article history:

Received 29 February 2008
Received in revised form 5 May 2008
Accepted 7 May 2008
Available online 13 May 2008

Keywords:

Artificial neural networks
Phase behaviour
Microemulsions
Labrasol®
Cremophor® RH 40
Plurol Isostearique®

ABSTRACT

The objective of this study was to develop artificial neural network (ANN) model suitable to predict successfully the borders of the microemulsion region in the quaternary system PEG-8 caprylic/capric glycerides (Labrasol®)/cosurfactant/isopropyl myristate/water, in order to minimise experimental effort. In our preliminary investigations of phase behaviour, two cosurfactants were used, PEG-40 hydrogenated castor oil (Cremophor® RH 40) and polyglyceryl-6 isostearate (Plurol Isostearique®). Microemulsion existence area in pseudo-ternary phase diagrams was determined using titration method at constant: (a) oil-to-water ratio ($\alpha = 50\%$, w/w); (b) surfactant-to-cosurfactant ratio (Km) 4:6; (c) Km 5:5; or (d) Km 6:4. It was found that the phase behaviour of systems involving polyoxyethylene type of cosurfactant depends significantly on oil-to-surfactant/cosurfactant mixture mass ratio (O/SCoS) but it is Km-independent. The formation of microemulsions in Labrasol®/polyglyceryl-6 isostearate based systems was a complex function of Km and O/SCoS and there was employed a Generalized Regression Neural Network (GRNN) with four layers as a predictive mathematical model, using data obtained from the phase behaviour study (the surfactant concentration in surfactant/cosurfactant mixture (S , %, w/w), the oil concentration in the mixture with tensides (O , %, w/w) as two input variables, and the water solubilization limit (W_{max} , %, w/w) as output data). After network training, six independent pairs of input/output data were used for network testing. The resulting GRNN was tested statistically and found to be of quality predictive power. This results confirmed that the trained GRNN could be effective in predicting the size of the microemulsion area providing valuable tool in formulation of this type of colloidal vehicles.

© 2008 Elsevier B.V. All rights reserved.

1. Introduction

During the last two decades, microemulsions are currently of interest to the pharmaceutical scientist as promising drug delivery vehicles due to their long term stability, ease of preparation, low toxicity and irritancy, considerable capacity for solubilization of a variety of drug molecules and great potential in bioavailability improvement (Bagwe et al., 2001; Gupta and Moulik, 2008; Lawrence and Rees, 2000; Malmstein, 1999; Spornath and Aserin, 2006). Microemulsion vehicles are thermodynamically stable and optically isotropic transparent colloidal systems consisting of water, oil and appropriate amphiphiles (surfactant, usually in combination with a cosurfactant), which formed spontaneously when admixing the appropriate quantities of the components. In water–oil–tensides systems, beside microemulsions, a diverse

range of other colloidal systems and coarse dispersions can be obtained, depending on temperature and physico-chemical properties and composition ratios of constituents. Range of water–oil–surfactant–cosurfactant compositions, which can form microemulsions at given temperature, as well as the effect of various formulation variables on a region of existence of microemulsions, usually determines from phase behaviour investigations and represents in phase diagrams (Kahlweit, 1999). Although phase diagrams represent detailed compositional maps which are of great interest to the formulators, it should be noted that the construction of complete phase diagrams requires complex and time consuming experimental work. Therefore, in order to overcome this issue and simplify the formulation of microemulsion-based drug-delivery systems there is a growing interest of researchers for *in silico* development of artificial neural network (ANN) models for prediction and/or optimization of the phase behaviour of microemulsion-forming systems using limited number of experiments and inputs (Agatonovic-Kustrin et al., 2003; Alany et al., 1999; Mendyk and Jachowicz, 2007; Richardson et al.,

* Corresponding author. Tel.: +381 11 395 1360; fax: +381 11 397 2840.
E-mail address: ljiki@pharmacy.bg.ac.yu (L. Djekic).

1997). An ANN is an intelligent non-linear mapping system built to loosely simulate the functions of the human brain. An ANN model consists of many nodes and their connections. Its capacity is characterized by the structure, transfer function and learning algorithms (Erb, 1993; Lippmann, 1987). Because of their model independence, non-linearity, flexibility, and superior data fitting and prediction ability, ANNs have gained interest in the pharmaceutical field in the past decade. ANNs have been used to solve various problems such as product development (Takayama et al., 2000), quantitative structure–activity relations (Huuskonen, 2003), prediction of the permeability of skin (Degim et al., 2003) and Caco-2 cells (Fujiwara et al., 2002), and prediction of drug stability (Ibrić et al., 2007).

Novel promising biocompatible microemulsion vehicles based on non-ionic surfactant PEG-8 caprylic/capric glycerides (Labrasol®), and polyoxyethylene or polyglycerol types of non-ionic tensides as cosurfactants, for oral (Ghosh et al., 2006) and transdermal delivery of drugs (Alvarez-Figueroa and Blanco-Méndez, 2001; Delgado-Charro et al., 1997; Djordjevic et al., 2004, 2005; Escribano et al., 2003; Kreilgaard et al., 2000; Rhee et al., 2001; Špiclin et al., 2003; Zhao et al., 2006) have been introduced recently. Despite the fact that the majority of these studies demonstrated the importance of the microemulsion systems composition for their properties and drug delivery potential, there have not been conducted previous systematic phase behaviour studies, and there were no general information about the influence of formulation variables on the microemulsion area. The results of our recent investigations (Djekic and Primorac, 2008) pointed out the possible effect of surfactant-to-cosurfactant mass ratio (Km) on the efficiency of Labrasol®/cosurfactant mixture to solubilize water and oil phase. Aside from Km value, the size of the microemulsion area may be dependent upon type and concentration of oil (Malcolmson et al., 1998; Warisnoicharoen et al., 2000).

The purpose of the experiments carried out in the present study was rapid screening of microemulsion area in the system containing Labrasol® (surfactant), PEG-40 hydrogenated castor oil or polyglyceryl-6 isostearate (cosurfactant), isopropyl myristate (oil) and water, conducting a small number of experiments. Therefore, in order of rationalisation, we investigated the effect of the cosurfactant type and the oil phase content on the water solubilisation capacity (W_{\max} , %, w/w) at selected values of Km, oil to surfactant/cosurfactant mixture mass ratio (O/SCoS), and mass fraction of the oil in the oil/water mixture (α , %, w/w). Furthermore, we used the obtained results to establish an appropriate ANN model suitable for prediction of microemulsion region boundary for any concentration of surfactant, cosurfactant and oil over a selected range of compositions.

2. Materials and methods

2.1. Materials

PEG-8 caprylic/capric glycerides (Labrasol®), and polyglyceryl-6 isostearate (Plurol Isostearique®), were a kind gift from Gattefosse, France. PEG-40 hydrogenated castor oil (Cremophor® RH 40) was obtained from BASF, Germany. Isopropyl myristate (Crodamol® IPM) was purchased from Croda Chemicals Europe, England. All chemicals were used as received without further purification. Water was double-distilled.

2.2. Phase behaviour investigations

The appropriate type of phase diagram for a full geometrical representation of a four component mixture at constant temperature is a tetrahedron (Fig. 1) in which each corner represents 100% of one

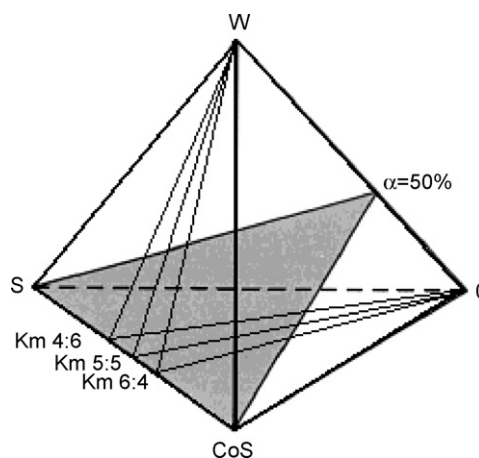


Fig. 1. Tetrahedron type of the phase diagram illustrating the position of the investigated pseudo-ternary phase triangles within the tetrahedron at $\alpha = 50\%$ (w/w) (the grey triangle), Km 4:6, Km 5:5 and Km 6:4, for the four component system Labrasol® (S)/cosurfactant (CoS)/isopropyl myristate (O)/water (W).

component of the system and each point inside the tetrahedron represents the one mixture of components at given percentages. Complete differentiation of quaternary mixtures which form microemulsion from others, would require a large number of experiments. Therefore, we selected four 'slices' within a tetrahedron (Fig. 1), where every 'slice' is in fact a pseudo-ternary phase triangle with two corners corresponding to 100% of two components and the third corner represents 100% of a binary mixture of two components at constant ratio, such as surfactant/cosurfactant or oil/water. The first pseudo-ternary phase diagram we constructed using a part of the results of our previous investigations of the influence of Km on the water and oil solubilization capacity in quaternary systems based on PEG-8 caprylic/capric glycerides (Djekic and Primorac, 2008), varying Km values from 1:9 to 9:1 at constant $\alpha = 50\%$ (w/w). Furthermore, in the present study, we selected three Km values (Km 4:6, Km 5:5 and Km 6:4) and determined pseudo-ternary phase diagrams in order to investigate more detailed the influence of O/SCoS value on microemulsion area.

2.2.1. Construction of pseudo-ternary phase diagrams at selected Km values

Three pseudo-ternary phase diagrams at constant Km were constructed using titration method at room temperature. Labrasol® and a cosurfactant were mixed to give the selected Km values. The obtained surfactant/cosurfactant mixtures were then mixed with isopropyl myristate at investigated O/SCoS ratios (1:9, 2:8, 3:7, 4:6, 5:5, 6:4, 7:3, 8:2, and 9:1). These mixtures were titrated dropwise with water, under moderate magnetic stirring. After addition of each aliquot of water, the samples were stirred to reach the equilibrium and checked visually. The transitions from turbid mixture to optically clear system, or from clear system to turbid dispersion were sharp. Clear, isotropic, one-phase systems were designated as microemulsions. In the present study, no distinction has been made between a microemulsion and a dispersion of micelles. The boundaries of the microemulsion domains were determined by titrating the isopropyl myristate/Labrasol®/cosurfactant mixtures with water, to the water solubilization limit (W_{\max} , %, w/w), which was detected as the transition from the isotropic single phase system to a two phase system (sample became turbid), upon addition of small amount of excess of water. The transparent samples containing W_{\max} were allowed to equilibrate for a minimum of 72 h and then examined visually for transparency and through crosspolarizers for optical isotropy.

2.3. Polarized light microscopy

In order to verify the isotropic nature of microemulsions, samples were examined using cross-polarized light microscopy (Leitz Wetzlar 307-083.103 514652, Germany). According to Friberg (1990), isotropic material, such as microemulsion, will not interfere with the polarized light.

2.4. Computational methods

We used commercially available Statistica Neural Networks (StatSoft, Inc., Tulsa, OK, USA) throughout the study. A Generalized Regression Neural Network (GRNN) was used for modelling and optimization of microemulsion boundary region. GRNNs are feed-forward networks comprised of four layers. The input layer comprises a variable number of neurons, which is equal to the number of independent features the network is trained on. The normalized input vector is copied onto the pattern units in the pattern layer, each representing a training case. An exponential activation function is applied, and the corresponding activation level is forwarded to the summation unit, where the density estimate of each pattern of each group or possible value is summarized. Finally, Bayesian theory is used to define the fourth layer.

Initially, in the radial layer, the number of hidden units varied from 1 to 27, using smoothing factor 0.01 and the *K*-means clustering algorithm. To select the optimal GRNN model, the observed versus predicted responses were shown in the regression plots drawn for the six test samples, which were excluded from training data set. The GRNN model that yielded a regression plot with a slope and squared correlation coefficient (r^2) that was closest to 1.0 was selected as the optimal GRNN model. A sum-squared error function was used in the network training. (The error is the sum of the squared differences between the target and actual output value on each output unit.)

Learned GRNN was used for modelling, simulation and optimization of the microemulsion boundary region in the following ways: testing experimental points in experimental fields; searching for the optimal solutions; presenting response surfaces (or contour plots).

3. Results and discussion

The microemulsion phase boundary for the investigated quaternary systems at $\alpha = 50\%$ (w/w) is mapped onto pseudo-ternary phase diagram in Fig. 2 (previously unpublished pseudo-ternary diagram). From the obtained diagram it can be seen the significant difference between the influence of polyoxyethylene and polyglycerol types of cosurfactants on the systems capacity to solubilize water and oil phase. Microemulsion area was larger in the presence of polyglyceryl-6 isostearate compared to PEG-40 hydrogenated castor oil, at $K_m > 3:7$. These results are in good agreement with the observation of Kunieda et al. (2002) and Fukuda (2005) that the solubilization capacity of polyglycerol surfactants is higher than that of polyoxyethylene surfactants due to the different solubility of polyglyceryl and polyoxyethylene chains in water and oil, resulting in more efficient adsorption of polyglycerol surfactants on the water/oil interface and the higher solubilization power. In the case of PEG-40 hydrogenated castor oil, microemulsion area decreases slightly at $K_m 5:5$, but in general, remains unchained significantly with K_m (Fig. 2). In the systems containing polyglyceryl-6 isostearate, it was observed increasing area of existence of microemulsions at the contents of the surfactant in the mixture with the cosurfactant higher than 30% (w/w) ($K_m > 3:7$), achieving a maximum at 50% (w/w) of the surfactant ($K_m 5:5$)

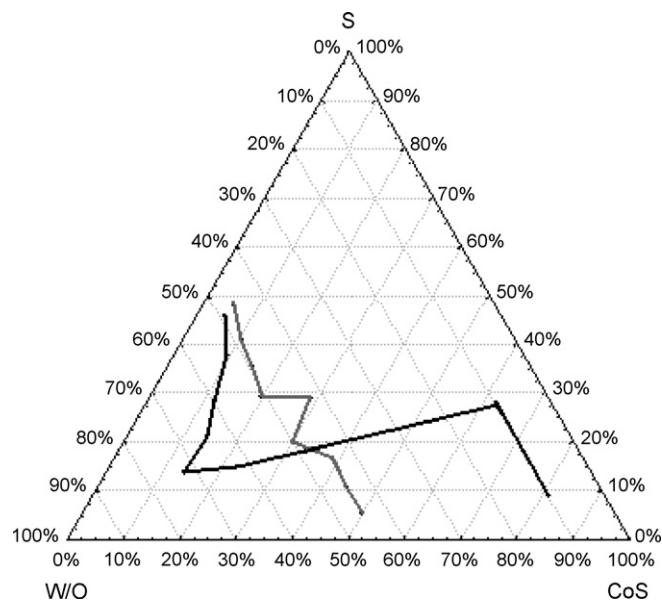


Fig. 2. Microemulsion area boundary in the pseudo-ternary phase diagram of the system Labrasol®/cosurfactant/isopropyl myristate/water at K_m values from 1:9 to 9:1, and constant $\alpha = 50\%$ (w/w) for polyglyceryl-6 isostearate (the black line) and polyoxyethylene-40 hydrogenated castor (the grey line) as cosurfactant (compositions to the right of the phase boundaries are microemulsions).

and diminishes with further increasing of K_m value. Based on the latter results, the complete microemulsion areas at $K_m 4:6$, $5:5$ and $6:4$ (at which would be expected large microemulsion regions of numerous potential self-microemulsifying drug delivery systems (SMEDDS) and microemulsions) were determined and presented in Figs. 3 and 4a–c. From the data shown in Fig. 3, in the systems based on Labrasol®/PEG-40 hydrogenated castor oil, it was confirmed that the influence of K_m on W_{max} was negligible. The area of microemulsion existence in the oil-rich systems was small, but increases as approaching the tensides-rich systems and there were observed continuous transformations from w/o

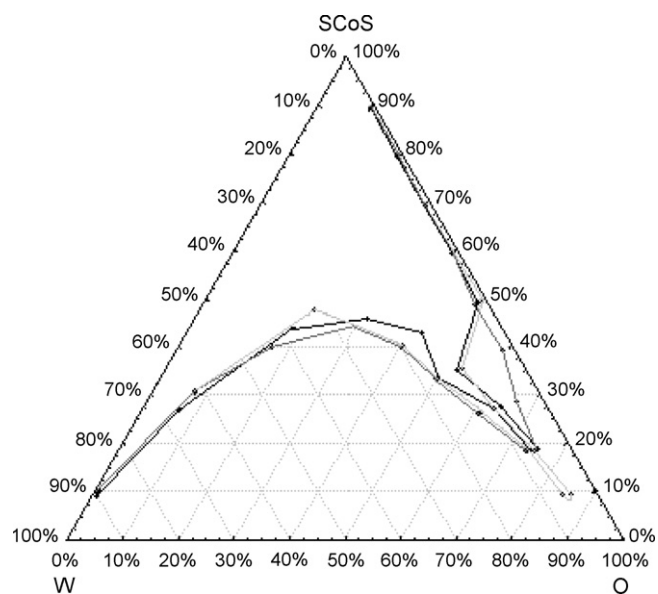


Fig. 3. The microemulsion area in pseudo-ternary phase diagram of the system Labrasol®/polyoxyethylene-40 hydrogenated castor oil/isopropyl myristate/water at $K_m 4:6$ (within the dark grey line), $K_m 5:5$ (within the light grey line) and $K_m 6:4$ (within the black line).

to o/w microemulsions (Fig. 3). On the contrary, in the systems containing polyglyceryl-6 isostearate the maximum percentage of water incorporated and the concentration range over which the microemulsion formed, varied depending upon K_m and $O/SCoS$. It is noticeable from Fig. 4a–c that there was a significant increase in the microemulsion region size as well as a diminution of the area of turbid systems within the microemulsion field when the ratio between the surfactant and the cosurfactant increases from 4:6 to 6:4. Also, the microemulsion area boundary widens as $O/SCoS$ become closer to 4:6 (at K_m 4:6 and K_m 6:4) and 5:5 (at K_m 5:5), while in the case of surfactant-rich systems ($O/SCoS > 6:4$) as well as oil-rich systems ($O/SCoS < 4:6$), W_{max} values were reduced (Fig. 4a–c). This can be explained by the possibility that the oil, isopropyl myristate, behaves as a ‘cosurfactant’ at relatively balanced ratio between oil and Labrasol®/polyglyceryl-6 isostearate mixture. This results were consistent with the previous observation that fatty acid esters

due to small molecular volume may act as cosurfactants penetrating the interfacial surfactant monolayer and subsequently affecting a solubilization capacity of the system (Malcolmson et al., 1998; Warisnoicharoen et al., 2000), but also indicated the importance of the nature of the surfactant/cosurfactant mixture and $O/SCoS$ value for the oil influence on the extent of microemulsion formation.

The results of the phase behaviour investigations pointed out that microemulsion boundary in the system Labrasol®/PEG-40 hydrogenated castor oil/isopropyl myristate/water was unaffected with the surfactant/cosurfactant ratio and unsurprisingly, W_{max} increases as $O/SCoS$ decreases, providing a quite clear information about possible microemulsions formulations over the whole investigated range of compositions. Phase behaviour of the system Labrasol®/polyglyceryl-6 isostearate/isopropyl myristate/water was much more complex and the obtained data were used to establish an appropriate ANN model which will describe

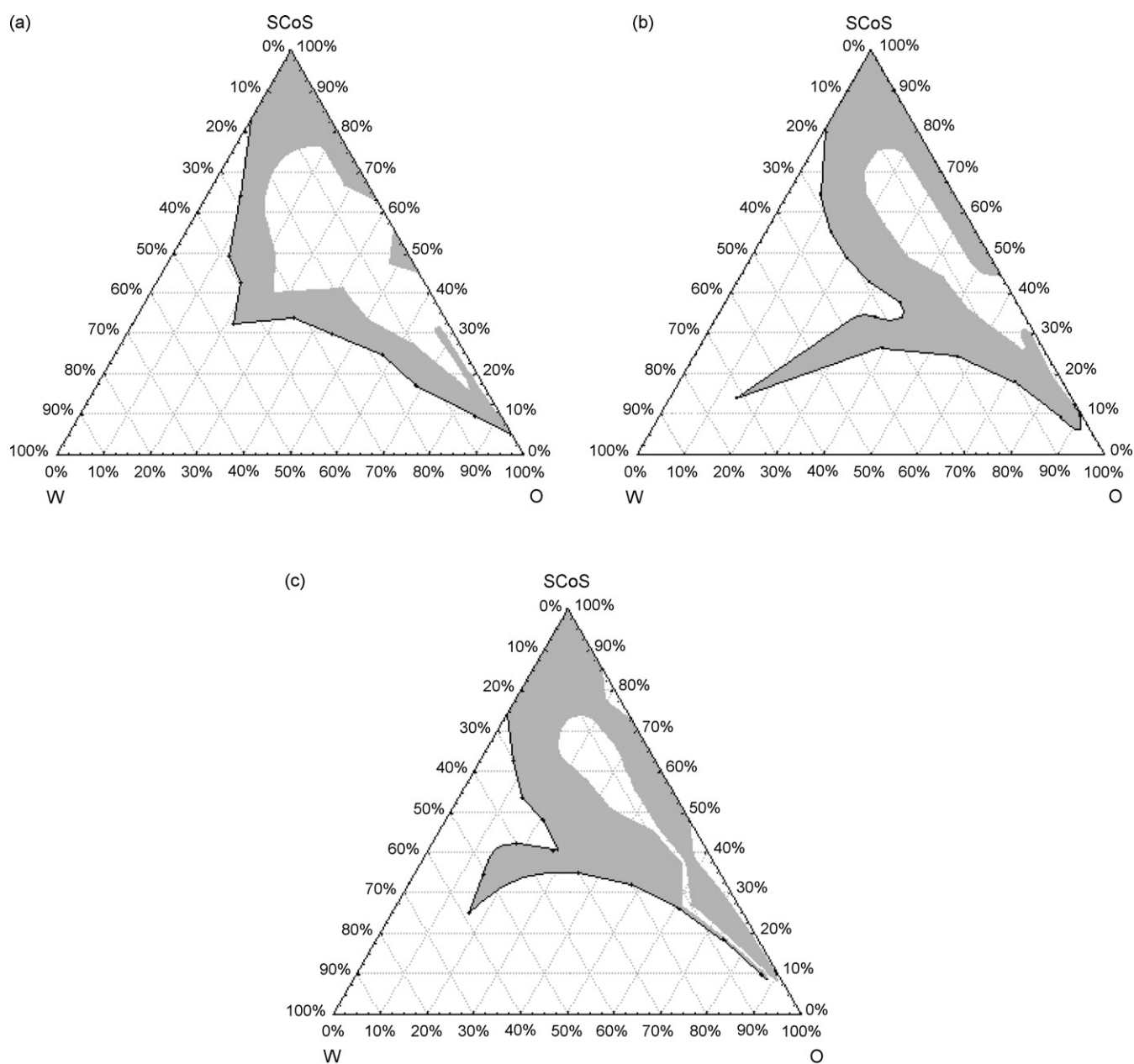


Fig. 4. Pseudo-ternary phase diagrams of the system Labrasol®/polyglyceryl-6 isostearate/isopropyl myristate/water at (a) K_m 4:6, (b) K_m 5:5 and (c) K_m 6:4 (grey fields represent the microemulsion area).

the relationships between compositional factors such as K_m and $O/SCoS$ and the size of the area of microemulsions.

The construction of the diagrams in Fig. 4a–c was based on a set of data from 27 independent titrations of oil/tensides mixtures with water (9 titrations at three K_m values). Furthermore, these experiments were used to generate the inputs and output for artificial neural networks training. The inputs were K_m values expressed as the surfactant concentration in surfactant/cosurfactant mixture (S , %, w/w) and $O/SCoS$ values expressed as the oil concentration in the mixture with tensides (O , %, w/w). The output was the water solubilization limit (W_{max} , %, w/w), which represents a microemulsion systems boundary for a given quaternary mixture. Additionally, 6 initial Labrasol®/polyglyceryl-6 isostearate/isopropyl myristate mixtures were randomly selected from the investigated area of the tetrahedron located between 40 and 60% (w/w) on the surfactant axis and 10–90% (w/w) on the oil axis (Table 1), and corresponding data together with the results of the water titration were used to test the ability of the trained network for prediction of phase behaviour.

A set of outputs and inputs was used as tutorial data and fed into the computer. A GRNN was chosen as the network type. The main advantage of GRNNs is that they involve a single-pass learning algorithm and are therefore much faster to train than the well-known back-propagation paradigm (Specht, 1990). Furthermore, they differ from classic neural networks in that every weight is replaced by a distribution of weights. This enables a large number of combinations of weights to be explored, and the exploration is less likely to end in a local minimum (Bruneau, 2001). Therefore, no test and verification sets are necessary and, in principle, all available data can be used for the network training. In a GRNN model, it is possible to select the number of units (nodes) in the second radial layer, the smoothing factor (which controls the deviation of the Gaussian kernel function located at the radial centres), and the clustering algorithm (e.g. subsampling, K -means or Kohonen). Several training sessions were conducted using different numbers of units in the hidden layer in order to determine the optimal GRNN structure. The learning period was completed when the minimum value of the root mean square (RMS) was reached:

$$RMS = \left[\frac{\sum (y_i^p - y_i^m)^2}{n} \right]^{1/2}$$

where y_i^p is the experimental (observed) response and y_i^m is the calculated (predicted) response and n is the number of experiments. The selected ANN structure had four layers: the first layer had two input units, the second layer had 27 hidden units (with negative exponential activation and radial postsynaptic function), the third layer had two units, and the fourth layer had one output unit (Fig. 5). Twenty-seven units in a hidden layer were needed to obtain an excellent prediction of the response variable.

Input values for test data were presented to the GRNN when network training was completed. RMS reached after the training was 0.9%, which is an acceptable value. Fig. 6 presents response

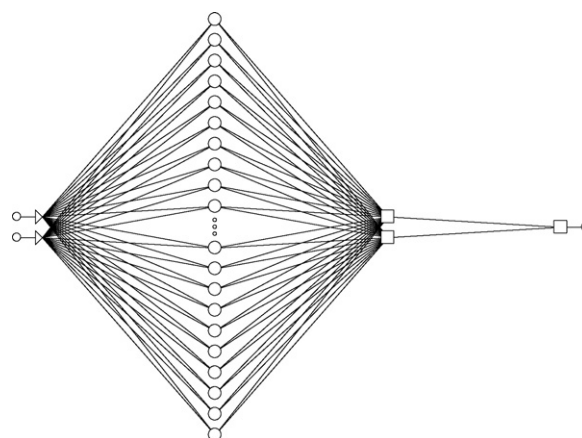


Fig. 5. The GRNN architecture used for the prediction of phase boundary for the investigated Labrasol® based microemulsions.

surface generated by GRNN presenting influence of the surfactant concentration in surfactant/cosurfactant mixture (S , %, w/w) and oil concentration in the mixture with tensides (O , %, w/w) on the water solubilization limit (W_{max} , %, w/w). Experimental and predicted values of W_{max} for the tested Labrasol®/polyglyceryl-6 isostearate/isopropyl myristate mixtures are presented in Table 1. It is possible, using this trained and tested GRNN network, to predict W_{max} for any combination of surfactant versus cosurfactant concentration (from 40 to 60%, w/w) and oil concentration (from 10 to 90%, w/w) in the initial surfactant/cosurfactant/oil mixture, without performing experiments. Important aspect of the presented experimental work is that input and output values were obtained from three pseudo-ternary phase diagrams which represent a part of the tetrahedron containing the largest microemulsion region and therefore the greatest number of potential microemul-

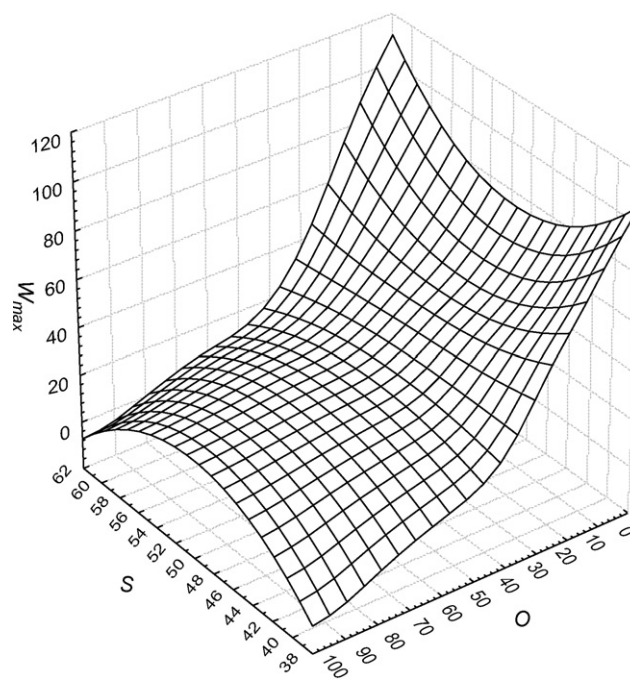


Fig. 6. Response surface presenting the influence of the surfactant concentration in surfactant/cosurfactant mixture (S , %, w/w) and the oil concentration in the mixture with tensides (O , %, w/w) on the water solubilization limit (W_{max} , %, w/w) which corresponds to a microemulsion region boundary for Labrasol®/polyglyceryl-6 isostearate/isopropyl myristate/water system.

Table 1
Experimental and predicted values of W_{max} for the test mixtures

S (% w/w)	O (% w/w)	W_{max} (% w/w)	
		Experimental values	Predicted values
45.00	35.00	30.26	33.24
43.00	65.00	30.36	32.25
55.00	25.00	32.98	34.47
48.00	75.00	13.04	10.10
45.00	40.00	31.32	32.55
43.00	70.00	34.21	34.47

sion formulations. Each phase triangle in Fig. 4a–c was constructed from only nine experiments (nine titrations). The applied titration method was useful to diminish the effort to collect data requested for GRNN determination, in contrast to alternative construction of phase diagrams by preparation of individual tensides/oil/water mixtures where the determination of all combinations of components which produce microemulsions is time consuming and requires huge number of individual experiments.

4. Conclusions

This study demonstrated the simplified experimental approach for investigation of phase behaviour of quaternary system Labrasol®/cosurfactant/isopropyl myristate/water using the titration method for the construction of complete pseudo-ternary phase diagrams and, additionally, developing GRNN model to understand the effect of formulation and compositional variables on the size and the position of microemulsion region. We found that microemulsion phase borders were independent of K_m in the presence of polyoxyethylene type of cosurfactant, while, polyglycerol ester cosurfactant generates very complex phase behaviour determined simultaneously by K_m and $O/SCoS$. In the present study have been successfully estimated combined influences of K_m and $O/SCoS$ within a predictive mathematical model which gives accurate predictions of microemulsion formation in Labrasol®/polyglyceryl-6 isostearate/isopropyl myristate/water. The GRNN model provided deeper understanding and predicting of water solubilization limit for any combination of surfactant concentration and oil concentration in their mixture, within the investigated range. The obtained results show that phase behaviour investigations based on titration method in combination with an optimized artificial neural network can provide useful tools which may limit the experimental effort for the formulation of pharmaceutically acceptable microemulsion vehicles.

Acknowledgements

The authors would like to thank to Ministry of Science of Republic of Serbia for financial support within the framework of the Project No. 142071B. Also, we would like to thank to Gattefosse s.a. and BASF for kindly supplying the samples of surfactants used in this study.

References

Agatonovic-Kustrin, S., Glass, B.D., Wisch, M.H., Alany, R.G., 2003. Prediction of stable microemulsion formulation for the oral delivery of a combination of antitubercular drugs using ANN methodology. *Pharm. Res.* 20, 1760–1764.

Alany, R.G., Agatonovic-Kustrin, S., Rades, T., Tucker, I.G., 1999. Use of artificial neural networks to predict quaternary phase systems from limited experimental data. *J. Pharm. Biomed. Anal.* 19, 443–452.

Alvarez-Figueroa, M.J., Blanco-Méndez, J., 2001. Transdermal delivery of methotrexate: iontophoretic delivery from hydrogels and passive delivery from microemulsions. *Int. J. Pharm.* 215, 57–65.

Bagwe, R.P., Kanicky, J.R., Palla, B.J., Patanjali, P.K., Shah, D.O., 2001. Improved drug delivery using microemulsions: rationale, recent progress, and new horizons. *Crit. Rev. Ther. Drug Carrier Syst.* 18, 77–140.

Bruneau, P., 2001. Search for a predictive generic model of aqueous solubility using Bayesian neural nets. *J. Chem. Inf. Comput. Sci.* 41, 1605–1616.

Degim, T., Hadgraft, J., Ilbasnis, S., Ozkan, Y., 2003. Prediction of skin penetration using artificial neural network (ANN) modelling. *J. Pharm. Sci.* 92, 656–664.

Delgado-Charro, M.B., Iglesias-Vilas, G., Blanco-Mendez, J., Lopez-Quintela, M.A., Guy, R.H., 1997. Delivery of a hydrophilic solute through the skin from novel microemulsion systems. *Eur. J. Pharm. Biopharm.* 43, 37–42.

Djekic, L., Primorac, M., 2008. The influence of cosurfactants and oils on the formation of pharmaceutical microemulsions based on PEG-8 caprylic/capric glycerides. *Int. J. Pharm.* 352, 231–239.

Djordjevic, L., Primorac, M., Stupar, M., Krajisnik, D., 2004. Characterization of caprylocaproyl macroglycerides based microemulsion drug delivery vehicles for an amphiphilic drug. *Int. J. Pharm.* 271, 11–19.

Djordjevic, L., Primorac, M., Stupar, M., 2005. In vitro release of diclofenac diethylamine from caprylocaproyl macroglycerides based microemulsions. *Int. J. Pharm.* 296, 73–79.

Erb, R.J., 1993. Introduction to backpropagation neural network computation. *Pharm. Res.* 10, 165–170.

Escribano, E., Calpena, A.C., Queralt, J., Obach, R., Domenech, J., 2003. Assessment of diclofenac permeation with different formulations: anti-inflammatory study of a selected formula. *Eur. J. Pharm. Sci.* 19, 203–210.

Friberg, S.E., 1990. Micelles, microemulsions, liquid crystals, and the structure of stratum corneum lipids. *J. Soc. Cosmet. Chem.* 41, 155–171.

Fujiwara, S., Yamashita, F., Hashida, M., 2002. Prediction of Caco-2 cell permeability using a combination of MO-calculation and neural network. *Int. J. Pharm.* 237, 95–105.

Fukuda, M., 2005. The importance of lipophobicity in surfactants: methods for measuring lipophobicity and its effect on the properties of two types of nonionic surfactant. *J. Colloid Interface Sci.* 289, 512–520.

Ghosh, P.K., Majithiya, R.J., Umrethia, M.L., 2006. Design and development of microemulsion drug delivery system of acyclovir for improvement of oral bioavailability. *AAPS Pharm. Sci.* 7 (Article 77, <http://www.aapspharmsci.org>).

Gupta, S., Moulik, S.P., 2008. Biocompatible Microemulsions and their prospective uses in drug delivery. *J. Pharm. Sci.* 97, 22–45.

Huuskonen, J., 2003. QSAR modelling with the electropological state indices: predicting the toxicity of organic chemicals. *Chemosphere* 50, 949–953.

Ibrić, S., Jovanović, M., Djurić, Z., Parojčić, J., Solomun, Lj., Lučić, B., 2007. Generalized regression neural network in prediction of drug stability. *J. Pharm. Pharmacol.* 59, 745–750.

Kahlweit, M., 1999. Microemulsions. *Ann. Rep. Prog. Chem. Sect. C* 95, 89–115.

Kreilgaard, M., Pedersen, E.J., Jaroszewski, J.W., 2000. NMR characterization and transdermal drug delivery potential of microemulsions. *J. Control. Release* 69, 421–433.

Kunieda, H., Akahane, A., Feng, J., Ishitobi, M., 2002. Phase behavior of polyglycerol didodecanoates in water. *J. Colloid Interface Sci.* 245, 365–370.

Lawrence, M.J., Rees, G.D., 2000. Microemulsion-based media as novel drug delivery systems. *Adv. Drug Deliv. Rev.* 45, 89–121.

Lippmann, R.P., 1987. An introduction to computing with neural nets. *IEEE ASSP Mag.* 4, 4–22.

Malcolmson, C., Satra, C., Kantaria, S., Sidhu, A., Lawrence, M.J., 1998. Effect of oil on the level of solubilization of testosterone propionate into nonionic oil-in-water microemulsions. *J. Pharm. Sci.* 87, 109–116.

Malmstein, M., 1999. Microemulsion in pharmaceuticals. In: Kumar, P., Mittal, K.L. (Eds.), *Handbook of Microemulsion: Science and Technology*. Marcel Dekker, New York, Basel, pp. 755–772.

Mendyk, A., Jachowicz, R., 2007. Unified methodology of neural analysis in decision support systems built for pharmaceutical technology. *Exp. Syst. Appl.* 32, 1124–1131.

Rhee, Y.-S., Choi, J.-G., Park, E.-S.K., Chi, S.G.-C., 2001. Transdermal delivery of ketoprofen using microemulsions. *Int. J. Pharm.* 228, 161–170.

Richardson, C.J., Mbanefo, A., Abofazel, R., Lawrence, M.J., Barlow, D.J., 1997. Prediction of phase behavior in microemulsion systems using artificial neural networks. *J. Colloid Interface Sci.* 187, 296–303.

Specht, D.F., 1990. Probabilistic neural networks. *Neural Networks* 3, 109–118.

Spornath, A., Aserin, A., 2006. Microemulsions as carriers for drugs and nutraceuticals. *Adv. Colloid Interface Sci.* 128–130, 47–64.

Špiclin, P., Homar, M., Zupančič-Valant, A., Gašperlin, M., 2003. Sodium ascorbil phosphate in topical microemulsions. *Int. J. Pharm.* 256, 65–73.

Takayama, K., Morva, A., Fujikawa, M., Hattori, Y., Obata, Y., Nagai, T., 2000. Formula optimization of theophylline controlled release tablet based on artificial neural networks. *J. Control. Release* 68, 175–186.

Warisnoicharoen, W., Lansley, A.B., Lawrence, M.J., 2000. Nonionic oil-in-water microemulsions: the effect of oil type on phase behaviour. *Int. J. Pharm.* 198, 7–27.

Zhao, X., Liu, J.P., Zhang, X., Li, Y., 2006. Enhancement of transdermal delivery of theophylline using microemulsion vehicle. *Int. J. Pharm.* 327, 58–64.